Quantum Computing with NMR: Deutsch-Josza and Grover Algorithms

Charles S. Epstein* and Ariana J. Mann
MIT Department of Physics
(Dated: March 14, 2012)

A Bruker Avance 200 NMR Spectrometer was used to perform simple quantum computations on a two quantum-bit (qubit) bulk system of $^{13}CHCl_4$. Base states $|00\rangle$ were created through the process of temporal averaging. The logic of the controlled-NOT (CNOT) gate was observed and used in the application of the Deutsch-Josza and Grover algorithms. The Deutsch-Josza algorithm was successfully used to determine whether the output of a two-bit function was constant or balanced. The Grover search algorithm, theoretically capable of completing a search in $O(\sqrt{N})$ time, was implemented and used to find the desired state in one iteration.

I. PROBLEM AND RELEVANT THEORY

I.1. Quantum Information Processing

Quantum computers, operating on quantum bits ("qubits"), are theoretically capable of performing a variety of computations in a faster order of time than their classical counterparts. This is made possible through the harnessing of quantum mechanical properties such as superposition, interference, and entanglement. For example, a quantum computer can determine whether the output of a two-bit function is constant or balanced in one evaluation with the Deutsch-Josza algorithm, akin to checking the fairness of a coin in one glance. Further, with the Grover search algorithm, a list can be searched in $O(\sqrt{N})$ time, a large speedup over the classical $O(N)$ time. Both of these provide examples of computational accelerations of which there is no known classical analog.

I.2. Controlled-NOT Gate

The Controlled-NOT (CNOT) logic gate is a crucial component of many quantum algorithms. It is similar to the classical XOR gate. CNOT maps the state $|x\rangle|y\rangle$ to $|x\rangle|y \oplus x\rangle$[1], where $\oplus$ refers to addition mod 2. The truth table is as follows:

TABLE I. CNOT Inputs and Outputs: Truth Table

Input State		Output State
$\|00\rangle$	$\rightarrow$	$\|00\rangle$
$\|01\rangle$	$\rightarrow$	$\|01\rangle$
$\|10\rangle$	$\rightarrow$	$\|11\rangle$
$\|11\rangle$	$\rightarrow$	$\|10\rangle$

If we define the state density matrix $\rho = |\psi\rangle\langle\psi|$, we can rewrite the CNOT gate as:

$$U_{cn} = \begin{bmatrix} 1 & 0 & 0 & 0 \\ 0 & 1 & 0 & 0 \\ 0 & 0 & 0 & 1 \\ 0 & 0 & 1 & 0 \end{bmatrix} \quad (1)$$

which acts upon ρ as a unitary transformation. As density matrices are a useful tool in the analysis of quantum information systems, this form of CNOT is important to note.

I.3. Deutsch-Josza Algorithm

Let us consider a function $f(x)$ that takes one bit as input and has one bit as output. There are four possible sets of outputs the function can have:

x	$f_1(x)$	$f_2(x)$	$f_3(x)$	$f_4(x)$
0	0	1	0	1
1	0	1	1	0

Functions $f_1(x)$ and $f_2(x)$ are *constant*, having the same output for a 0 or 1 input bit, and functions $f_3(x)$ and $f_4(x)$ are *balanced*, having different outputs. Classically, one would expect a requirement to check both inputs of the function to determine if it is constant or balanced, corresponding to two iterations of an algorithm. With a quantum computer, however, the function need only be evaluated once, on a superposition of all possible inputs. First, we implement these functions U_{fk} as $|x\rangle|y\rangle \rightarrow |x\rangle|y \oplus f_k(x)\rangle$. Thus, they take the form:

- f_1: $|x\rangle|y\rangle \rightarrow |x\rangle|y\rangle$: Identity
- f_2: $|x\rangle|y\rangle \rightarrow |x\rangle|y \oplus 1\rangle = |x\rangle|\neg y\rangle$: NOT y
- f_3: $|x\rangle|y\rangle \rightarrow |x\rangle|y \oplus x\rangle$: CNOT gate
- f_4: $|x\rangle|y\rangle \rightarrow |x\rangle|y \oplus \neg x\rangle$: NOT x, CNOT gate, NOT x

With these functions, the Deutsch-Josza algorithm can be implemented as follows:

1. Acquire base state $|00\rangle$

* cepstein@mit.edu

[1] In this paper, we refer to a two-qubit state as $|xy\rangle$, $|x\rangle|y\rangle$, or $|x\rangle \otimes |y\rangle$, with $(x, y) \in \{0, 1\}$, as equivalent methods of notating a state in the two-spin Hilbert space.

2. Set up superposition with a Hadamard transform. This translates the base state into the maximally-mixed superposition state

$$\frac{1}{2}\left[|00\rangle - |01\rangle + |10\rangle - |11\rangle\right]$$

in an invertible way.

3. Act with U_{fk}. Note that it acts on the maximally-mixed state, thereby evaluating all possible inputs at once.

4. Undo the superposition with an inverse Hadamard transform. This breaks down the superposition in a deterministic and invertible way, bringing us back to a pure state.

5. Measure the output state. We note that the state takes the form[1]

$$\frac{1}{2}[((-1)^{f(0)} + (-1)^{f(1)})|0\rangle + (-(-1)^{f(0)} + (-1)^{f(1)})|1\rangle] \otimes |0\rangle$$

which reduces to $|00\rangle$ if $f(0) = f(1)$ (f is constant), or $|10\rangle$ if $f(0) \neq f(1)$ (f is balanced).

I.4. Grover Search Algorithm

The Grover search algorithm allows a list to be searched in $O(\sqrt{N})$ time. Consider a function $f(x)$ that always maps to zero unless $x = x_0$, in which case the function maps to one. To classically search a list of four elements for the value x_0 takes an average of 2.25 evaluations of the function. A four-element list corresponds to a 2-qubit system, within which the value x_0 can be found in only one evaluation.

The Grover iteration consists of the sequence of operations $G = H^{\otimes 2}PH^{\otimes 2}O$. O is an "oracle" operator that flips the phase of the basis element of the state corresponding to x_0. For $x_0 = 2$, corresponding to a desired state of $|10\rangle$, this takes the form $\rho = \mathrm{diag}(1, 1, -1, 1)$. P is a conditional phase-shift operator that takes the form $\rho = \mathrm{diag}(1, -1, -1, -1)$ [1]. Furthermore, $H^{\otimes 2}$ is the Hadamard transform applied to both qubits.

We apply the Grover iteration to the base state $|\psi_0\rangle = H^{\otimes 2}|00\rangle$ any number of times k. Thus, we define $|\psi_k\rangle = G^k|\psi_0\rangle$. We expect the sequence $G|\psi_0\rangle$ to produce the x_0 state $|10\rangle$. The Grover algorithm also has a characteristic oscillatory behavior resulting from the perdiodicity of $\langle x_0|\psi_k\rangle$[1]. We find an oscillation period of 3, as the output state rotates between the desired state and the base state $|00\rangle$. Thus we also expect the to find the state $|10\rangle$ after four iterations of the Grover sequence.

I.5. Quantum Computing with NMR

A simple yet effective way of implementing a quantum computer is through the use of a nuclear magnetic resonance (NMR) spectrometer. This works under the following principle: within a sample immersed in a magnetic field, a small fraction of the spins will invariably be aligned along the magnetic field due to the lower energy of the aligned state. A spin perturbed from this equilibrium will precess around the magnetic field at the Larmor frequency. In the technique of pulsed-NMR, a well-tuned radio-frequency (RF) pulse near the Larmor frequency in a direction $\hat{x}$ causes the spins to precess about that axis for the length of the pulse. If timed precisely, the RF pulse can cause a 90° rotation, in which the $\hat{z}$-aligned spins rotate 90° into the $x-y$ plane. The subsequent precession causes an oscillating magnetic field with a large enough amplitude to be detected with a pickup coil. As the sample relaxes back to equilibrium, the magnitude of the signal decays in what is called a free-induction decay (FID). The Fourier transform of the FID provides a spectrum with Lorentzian peaks at the Larmor frequencies of the spins in the sample.

For a two-spin system, four peaks are observed. The peaks of each spin are split by a frequency J due to a coupling: if one qubit is spin-up, the magnetic field at the other qubit is lowered, causing the oscillation frequency to drop slightly. The opposite is true as well. Furthermore, if the state of the system is given by the density matrix $\rho = \mathrm{diag}(a, b, c, d)$, then the resulting peak integrals will be $\{a - c, b - d\}$ for qubit 1, and $\{a - b, c - d\}$ for qubit 2.

Ideally, quantum computations are performed on a pure base state $|00\rangle$ where $\rho_{base} = \mathrm{diag}(1, 0, 0, 0)$. A drawback of NMR quantum computing is that pure base states can be difficult to obtain, as the sample is at room temperature and entropy is high. The thermal density matrix can be calculated using statistical mechanics [1]:

$$\rho = \frac{e^{\beta H}}{\mathcal{Z}}$$

where $\beta = 1/k_B T$ and $\mathcal{Z}$ is the partition function. Thus, the thermally expected density matrix is

$$\rho_{therm} = \frac{I}{4} + 10^{-4}\begin{bmatrix} 5 & 0 & 0 & 0 \\ 0 & 3 & 0 & 0 \\ 0 & 0 & -3 & 0 \\ 0 & 0 & 0 & -5 \end{bmatrix} \tag{2}$$

This corresponds to qubit 1 peak integrals both having magnitude 8×10^{-4}, and qubit 2 peak integrals of 2×10^{-4}. This is unacceptable for performing quantum computations as it is a highly mixed state. The process of temporal averaging was used to construct pseudopure states, allowing us to observe the effects of quantum algorithms on an effective basis state. In this process, the

algorithm of interest is implemented three times, each following the application of a series of permutations. The permutations are chosen such that when the three final states are averaged, the result is close to that which would result from the application of the pulse sequence to a pure base state.

II. EXPERIMENTAL SKETCH AND SALIENT DETAILS

II.1. Setup Overview

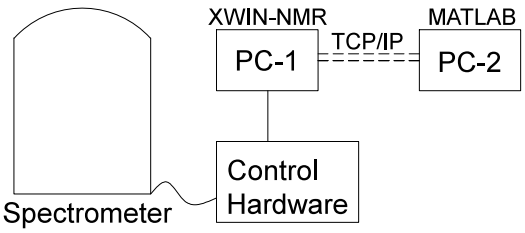

FIG. 1. Block diagram of the experimental setup

A Bruker Avance 200 NMR Spectrometer was used in this experiment. This spectrometer houses a 4.7 Tesla cryogenically cooled superconducting electromagnet. The cryogenic system consisted of a liquid helium core with a liquid nitrogen jacket. The magnetic field was "shimmed" by a number of correction coils that allow the field along various spherical Legendre polynomials to be adjusted in order to cancel gradients that can lead to decoherence. The magnetic field is capable of being shimmed to a uniformity of 10^{-9} over 1 cm^3. The sample, $^{13}CHCl_3$ (carbon-13 chloroform), was located in a flame-sealed 5mm glass tube in a "spinner" at room temperature inside the spectrometer. The spinner provided a means for the sample to be spun at a fast rate in order to average away the transverse inhomogeneities of the magnetic field.

The hardware controlling the spectrometer was connected to a Linux computer running Bruker's xwin-nmr software. A second computer, an Athena workstation, was connected via direct TCP/IP link to other machine. Commands were sent through a MATLAB script that translated them into *nmrx* commands to be sent over the network link. This provided a suite of available commands, including the specification of pulse lengths, directions, phase corrections, and delays in arbitrary custom sequences.

The proton and carbon-13 of the $^{13}CHCl_3$ provided two fermionic particles to serve as qubits 1 and 2, respectively. The relaxation constants T_1 and T_2^* were measured to be 17.3 ± 0.2 s and 1.34 ± 0.16 s, respectively, for the proton, and for the carbon, $T_1 = 14.8 \pm 0.3$ s and $T_2^* = 1.88 \pm 0.18$ s. For comparison, the pulse sequences were on the order of milliseconds. T_1 was measured with the $180 - 90$ inversion-recovery method, and T_2^* was found from a fit to the Lorentzian peaks, which have width $2/T_2^*$. As a result of these relaxation times, 50 seconds were waited before the application of a pulse sequence in order to ensure the system had returned to equilibrium. A 90° pulse around the $\hat{x}$ axis was applied in order to initiate a readout FID.

III. DATA PRESENTATION AND ERROR ANALYSIS

In the following sections, we refer to pulse sequences with the capital letter of the corresponding qubit and the subscript of the rotation axis. For example, X_i is 90° rotation around $\hat{i}$ ($\hat{x}$) on qubit X, and $Y_{\bar{j}}$ is 90° rotation around $-\hat{j}$ ($-\hat{y}$) on qubit Y. A τ refers to a delay of time $1/2J = 2.325$ ms. The peak separation ($J = 215.05 \pm 0.01$ Hz) was measured by a simple subtraction; the sharpness of the peaks made one data point clearly the highest beyond poisson uncertainties, eliminating the necessity to fit a functional form.

The pulse widths were determined by measuring peak area as a function of pulse width, fitting to a decaying sinusoid, and finding the maximum. They were 9.32 ± 0.11 μs for the proton, and 10.04 ± 0.19 μs for the carbon.

For most implementations, only the proton spectrum was obtained due to the ease of reconstructing the state solely with its information. A positive peak refers to spin-up ($|0\rangle$), while a negative peak refers to spin-down ($|1\rangle$). Furthermore, a peak on the left indicates that the other qubit was spin-up, while a peak on the right indicates the other qubit was spin-down. As a result, a positive peak on the left refers to $|00\rangle$, and on the right, $|01\rangle$. A negative peak on the left refers to $|10\rangle$ and on the right, $|11\rangle$.

III.1. CNOT Gate

As an approximation to the CNOT gate, tests begun with the use of a near-CNOT gate. This gate is less error-prone as it only contains two pulses and one delay in the sequence $X_{\bar{j}} - \tau - X_i$. However, the phases differ for each qubit, i.e., the phase is not global. This makes it unsuitable for use in algorithms and causes a quicker accumulation of error. The near-CNOT gate is useful as a measure to estimate the uncertainties inherent in acquiring spectra.

Applying a near-CNOT gate on the $|00\rangle$ state yields the $|00\rangle$ state with real peak integrals for the proton of $(1.81, 0.25)$.[2] For carbon, the raw peaks are $(0.326, 0.057)$. These must be adjusted because of differences in amplifier gain; they should be set such that

[2] On peak integrals we exclude an arbitrary factor of 10^6 for clarity.

the proton peaks in the thermal spectrum have four times the area of the carbon peaks, as dictated by Eq. 2. Thus, after analysis of the thermal spectrum, it was determined that the carbon peaks should be multiplied by 3.46, yielding: $(1.13, 0.20)$. Solving the equations relating the elements of the density matrix and the peak integrals in a least-squares fashion yields:

$$\rho = \mathrm{diag}(0.791, 0.190, 0.019, 0.000)$$

where we stipulate that every element be positive and we normalize such that the trace is unity. Each element has an associated systematic error of 0.106, assigned as a result of compounding uncertainties from the the peak phases, pulse widths, and Lorentzian width (inhomogeneity). A more detailed explanation of this error can be found in Section III.4. The expected density matrix has only one element, one, at $|00\rangle$. Thus, the mean deviation of the matrix elements from the expected $\rho = \mathrm{diag}(1, 0, 0, 0)$ is 0.985σ. This effectively quantifies the error introduced by the non-zero secondary peaks.

The true CNOT gate can be translated into the pulse sequence $X_j Y_{\bar{j}} Y_{\bar{i}} Y_j X_{\bar{j}} X_{\bar{i}} X_{\bar{j}}$-$\tau$-$X_{\bar{j}}$ which replicates the unitary transformation matrix up to an irrelevant overall phase [2]. The output was just as expected, following Table I.

III.2. Deutsch-Josza Algorithm

The Hadamard operator can be translated to the pulse sequence $Y_j X_{\bar{j}}$. Further, the four functions U_{fk} can be translated as follows:

1. No pulses
2. NOT y: Y_i^2
3. CNOT: $X_j Y_{\bar{j}} Y_{\bar{i}} Y_j X_{\bar{j}} X_{\bar{i}} X_{\bar{j}}$-$\tau$-$X_{\bar{j}}$
4. NOT x, CNOT, NOT x: $X_i^2 X_j Y_{\bar{j}} Y_{\bar{i}} Y_j X_{\bar{j}} X_{\bar{i}} X_{\bar{j}}$-$\tau$-$X_{\bar{j}} X_i^2$

We recall that for a constant Function (f_1, f_2), we expect the state $|00\rangle$; for a balanced function (f_3, f_4), we expect $|10\rangle$. As can be seen in Fig. 2, this is clearly the case.

III.3. Grover Search Algorithm

The Grover sequence corresponding to a desired state of $|10\rangle$ can be represented by the pulse sequence $U = X_{\bar{i}} X_{\bar{j}} Y_{\bar{i}} Y_{\bar{j}} - \tau - X_{\bar{i}} X_{\bar{j}} Y_{\bar{i}} Y_{\bar{j}} - \tau$, according to [3]. Application of this algorithm G to the $|\psi_0\rangle$ state yields the state $|10\rangle$, as desired. Furthermore, $G^2|\psi_0\rangle$ yields $|00\rangle$, $G^3|\psi_0\rangle$ yields the mixed state, and $G^4|\psi_0\rangle$ gives $|10\rangle$ once again. This is in accord with the expected oscillatory behavior. Spectra can be seen in Fig. 3.

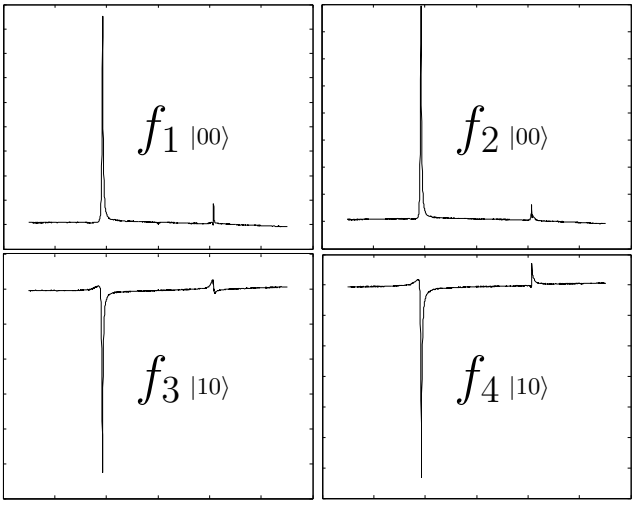

FIG. 2. Proton Spectra for Deutsch-Josza Algorithm. Axis labels removed for clarity. Y-axis is amplitude in arbitrary units, 5 height-units per tick. X-axis is frequency (Hz), 100 Hz per tick.

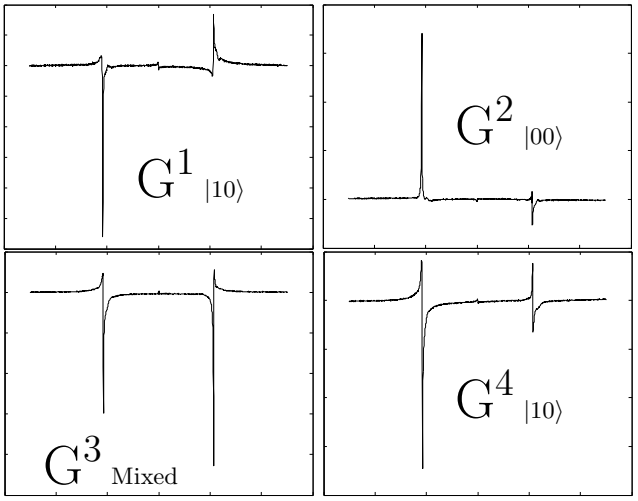

FIG. 3. Proton spectra from Grover algorithm output. Axis labels removed for clarity. Y-axis is amplitude in arbitrary units, 5 height-units per tick. X-axis is frequency (Hz), 100 Hz per tick. Note the less-pure states resulting from the longer Grover pulse sequences as well as the diminishing peak amplitudes.

III.4. A Note on Uncertainties

Pulse-width calibration error contributed approximately a 2.8% error for every 10 pulses, based on translating the uncertainty in the width measurement into an angle drift and then a peak area shift. Errors in the phases contributed a peak area uncertainty of approximately 9.5%, based on the size of the imaginary parts of the peaks after they had been minimized in a daily calibration. Further, magnetic field inhomogeneity, thereby variations in T_2^*, contribute approximately 9% error based on the uncertainty in peak width. Adding these in quadrature leads to an overall systematic uncertainty of approximately 13.4% within a spectrum. Day-

to-day magnetic field drift caused frequent reshimming to be necessary, increasing our errors further in a less quantifiable way. Qualitatively, it is almost always clear to which state a spectrum refers.

Typical secondary peaks have area less than 10% of the primary peak (i.e., Fig. 2). The secondary peaks observed in the implementation of the Grover algorithm are generally larger and asymmetric. This is likely a result of a cumulative phase error made apparent by the longer pulse sequences.

IV. CONCLUSIONS

The CNOT logic gate was implemented and followed the expected truth table. The Deutsch-Josza algorithm was implemented and used to test if a function was constant or balanced in one step. The Grover search algorithm was implemented and used to find a desired state among two qubits in one evaluation. The algorithmic speedup provided by quantum computation was thus shown.

[1] Junior Lab Staff, "Quantum Information Processing with NMR: MIT 8.14 Lab Guide," (2010).
[2] N. Gershenfeld and I. Chuang, Science **275**, 350 (1997).
[3] I. Oliveira *et al.*, *NMR Quantum Information Processing* (Elsevier Science, 2007).

ACKNOWLEDGMENTS

The author gratefully acknowledges his lab partner Ariana Mann for her equal part in the execution and analysis of this experiment.